Photocatalytic degradation of the pharmaceuticals *Paracetamol* and *Chloramphenicol* by Ln–modified ZnO photocatalysts

N. Kaneva, A. Bojinova[*], K. Papazova, D. Dimitrov

Laboratory of Nanoparticle Science and Technology, Department of General and Inorganic Chemistry, Faculty of Chemistry and Pharmacy, University of Sofia, 1164 Sofia, Bulgaria

Ln-modified (Ln = La, Ce, Eu) zinc oxide powders are synthesized by green thermal method. The materials are characterized by various techniques such as XRD, BET, TEM, SEM, EDX and UV-visible spectroscopy. The photocatalytic activity of the nanostructured ZnO modified with different rare earths is tested in the photodegradation of the commonly used drugs *Paracetamol* and *Chloramphenicol* in aqueous solution under UV light illumination. Highest degradation efficiencies are encountered for the materials modified with La^{3+}, degradation efficiencies values of 95.88% (*Paracetamol*) and 80.74% (*Chloramphenicol*) are achieved after 240 min of photocatalytic treatment. The photodegradation efficiency of doped ZnO powders follows the order La>Eu>Ce. This trend is observed in the course of degradation of both drugs (*Paracetamol* and *Chloramphenicol*). a_bojinova@hotmail.com

Keywords: rare earth, zinc oxide, *Paracetamol*, *Chloramphenicol*, photocatalytic degradation

INTRODUCTION

Pharmaceuticals and personal care products are a group of emerging environmental contaminants, which induce physicochemical and physiological effects in humans at low doses [1,2]. The latter distinguish them as unique group of contaminants from other contaminants like the persistent organic pollutants. Active pharmaceutical ingredients were detected in environment since 1970, when the first studies on drug contaminated domestic wastewaters were published [3,4] .An increasing number of investigations confirmed the presence of various pharmaceuticals and personal care products (PPCPs) in different environmental compartments worldwide [5] at low concentrations (ng L^{-1} to μg L^{-1}), but their input into the environment is continuous. Despite that most of the data, reported in literature, concern the occurrence of drugs of each therapeutic class in the aquatic environment, several reviews [6-8] mainly concern their attention on therapeutic classes detected in environment, presenting data collected from 134 articles published between 1997 and 2009 (Fig. 1). . The data is useful to find out the most appropriate active substances for ecotoxicity tests. According to data present in literature, scientific community has mainly concerned their attention on therapeutic classes such as, non-steroidal anti-inflammatory drugs, blood lipid lowering agents, antibiotics and sex hormones. By these reasons, this paper will focus in drugs belonging to those therapeutic classes. Non-steroidal anti-inflammatory drugs sold in high quantities without a prescription, .are used as pain killers in veterinary and human medicine. The antibiotic substances consumption worldwide is in hundreds of thousands of tons annually. In veterinary medicine, more than 70% of all consumed pharmaceuticals are antibiotics, and ∼6% in human medicine.

Pharmaceuticals are structurally designed to maximize their biological activity at low concentrations and developed to produce a prolonged action and have continuous everyday release to the environment [9]. These properties highlight the risks associated with the inadvertent presence of PPCPs in the environment. It has become a major concern because PPCPs are extensively and increasingly used in modern life, human and veterinary medicine and have continuous everyday release to the environment [9]. Therefore a priority pollutant lists have been developed by the European Union and by the United States Environmental Protection Agency, pointing a variety of contaminants present in wastewaters, storm water runoff and surface water. There is a lack of data on the toxicological implications in both target and non-target organisms after chronic exposure to complex mixtures of PPCPs at sub-therapeutic levels [9]. Much research is needed to characterize the influence of such exposure also on the public health status in the contaminated geographic areas. Further investigation is needed to provide more detailed definition of seasonal variations of PPCPs and their bioaccumulation in aquatic organisms [11].

* To whom all correspondence should be sent:
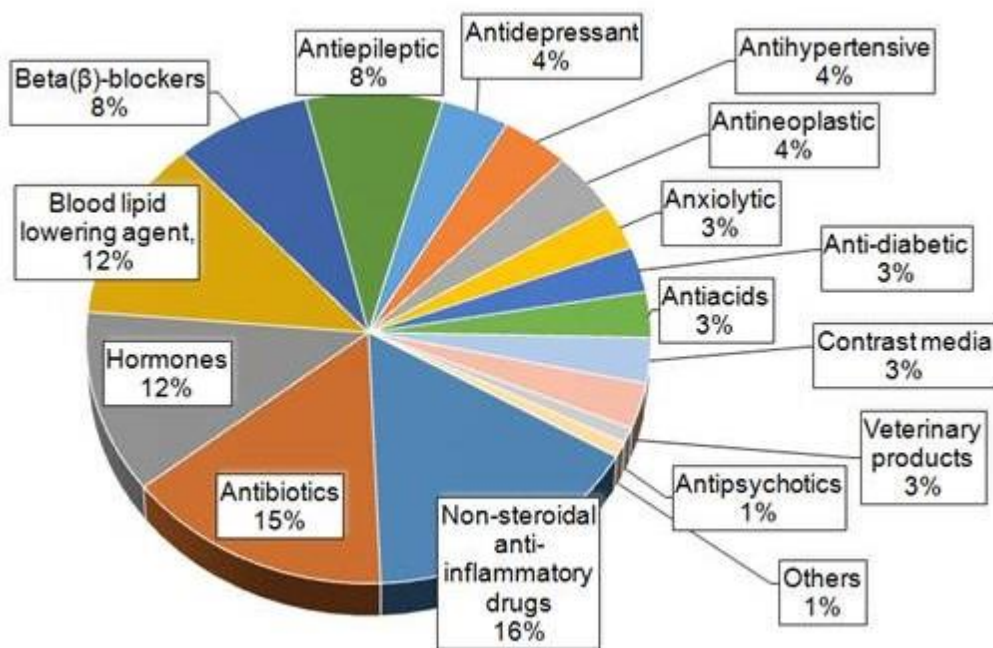E-mail: a_bojinova@hotmail.com

Fig. 1. Relative percentage of the most detected in the surface and groundwater therapeutic classes.

Some researchers [12-14] initially highlight the importance and further study on possible bioaccumulation by aquatic biota, including its implications for human exposure via consumption of contaminated fish or shellfish.

For this study, we selected commonly used pharmaceuticals with high volumes of production that have already been detected in the aquatic environment and in wild animals - anti-inflammatory antipyretic *paracetamol* (PCA) and antibiotic *chloramphenicol* (CA).

Photocatalysis, as advanced oxidation process, seems an efficient approach for purification of drugs contaminated waters using UV-irradiated inorganic oxides [15-19]. Zinc oxide and titania are the metal oxides, most widely used as photocatalysts. In comparison to TiO_2, in case of ZnO the lifetime of photogenerated electrons is significantly higher and the rate of recombination is lower, making ZnO an attractive material for photocatalytic applications [20]. Therefore this work is focused on photocatalysis with doped ZnO powders.

This study is a part of our greater investigation on lanthanide doped ZnO photocatalysts. The previous parts refer to: degradation of Malachite Green and Reactive Black 5 (at dye concentrations of 3, 5, 7 and 10 ppm) by doped with 0.5 and 1 % La ZnO nanoparticles, prepared by sol-gel method [21]; photocatalytic mineralization of 20 ppm Reactive Black 5 in natural Black Sea water [22]; photo-oxidation of ethylene in air as gas-phase

model pollutant with Ln-doped (Ln = La, Ce, Eu) ZnO powders [23].

EXPERIMENTAL
Reagents and materials

The commercial oxide powders: ZnO (>99.0 %) and ethanol absolute grade (99.5%) were supplied from ACROS Organics; La_2O_3 (>99.0 %), Eu_2O_3 (>99.0 %) and $Ce(NO_3)_3 \cdot 6H_2O$ (>99.0 %) were purchased from Fluka. All the solutions, used in the experiments, were prepared with distilled water.

The commercially available drugs *Paracetamol* (λ_{max} = 243 nm, ≥ 99.0% purity) and *Chloramphenicol* (λ_{max} = 278 nm, ≥ 99.0% purity) from Actavis were chosen as model contaminants for the photocatalytic water purification tests. A brief description of the investigated commonly used pharmaceuticals is given below.

Paracetamol is classified as a mild analgesic. It is commonly used for the relief of headaches and other minor aches and pains and is a major ingredient in large number cold and influenza remedies. In comparison to other over the counter pain relievers, *Paracetamol* is significantly more toxic in case of overdose [24, 25]. Some of its side effects are pointed in Table 1.

Chloramphenicol is broad-spectrum antibiotic. It is active against both Gram-positive and Gram-negative bacteria and against numerous groups of microorganisms as well. CA acts through inhibition of the microorganism protein synthesis and therefore is effective for treatment of number of

infectious diseases. The latter and its low cost and availability, made *Chloramphenicol* extensively used for most eye and ear infections cure and for treatment of domestic animals [26. However, the drug is associated with serious toxic effects in humans [27,28] (Table 1). This is the reason why *Chloramphenicol* usage in food-producing animals is banned in lots of countries and EU [29].

Table 1. Side effects of *paracetamol* and *chloramphenicol*

Pharmaceutical	Side effects	
	High doses	Prolonged use
Paracetamol $C_8H_9NO_2$	Hepatotoxicity, skin, liver and kidney damage,	Change the effect of other pharmaceutical drugs (rifampicin, cimetidine, chloramphenicol, busulfan)
Chloramphenicol $C_{11}H_{12}Cl_2N_2O_5$	Violations of blood-forming apparatus; haemolytic anemia leukemia, nausea, vomiting, diarrhea, stomatitis (gastrointestinal) reactions, headache, depression (neurotoxic effects), rash, itching, burning, redness, swelling, fever (allergic).	The development of fungal infections and resistance of microorganisms to the product

Catalysts modification and characterization

Three series of Ln- modified ZnO powders were prepared by simple and green thermal method (using simple preparation conditions and reduced synthesis time, with stable natural and nontoxic reagents, without any chemical residue after preparation of the samples). In our previous investigation it was experimentally found out that 2 mol% Ln content in the modified ZnO was optimal is for the mineralization of organic dye Reactive Black 5 [22]. Therefore, here we applied the same composition for photopurification of water from drugs contamination. For preparation of Ln-ZnO photocatalysts, calculated amounts of La_2O_3 (respectively Eu_2O_3 or $Ce(NO_3)_3.6H_2O$) and ZnO, corresponding to 2 mol% Ln content, were mixed thoroughly. Then small quantity of ethanol (~1-1.5 ml per g sample) was added as medium for more complete mixing to ensure intimal contact between the particles of both oxides. The initial charge was mixed for 10 min, then treated for 30 min by ultrasound (ultrasonic bath IKEDA RIKA 100 V 50/60Hz) and dried finally for 1 h at 100°C in order to obtain fine Ln-ZnO powders for photocatalysis. Each series of powder photocatalysts – La, Eu and Ce modified ZnO were prepared by repetition of the same procedure at the same dopants concentration - 2 mol%.

The surface area of pure and Ln-modified ZnO powders was estimated with BET analysis (N_2 adsorption). Prior the BET analysis, the samples were degassed for 4 h at 150°C before the N_2 adsorption. Pure ZnO and Ln-modified ZnO surfaces morphology was investigated by SEM (JSM-5510 JEOL operated at acceleration voltage of 10 kV). The elemental analysis and chemical characterization of the samples surface were performed by energy-dispersive X-ray spectroscopy via Quantax200 EDX detector, Bruker Resolution 126 eV. The crystallinity and phase composition of the catalysts were analyzed by X-ray diffraction (diffractometer Siemens D500 with Cu Kα radiation within 2θ range 25–40° at a step of 0.05°2θ and counting time 2 s/step). The average crystallite sizes were calculated by Scherrer's equation:

$$d_{hk}1 = k.\lambda/\beta.\cos(2\theta) \qquad (1)$$

where d_{hkl} is the average crystallite size (nm), λ is the wavelength of CuKα radiation ($\lambda = 0.154056$ nm), θ is the Bragg's diffraction angle, β is the full-width at half maximum intensity of the main characteristic peak (at 2θ converted to radians) and k is a constant ~0.9.

Photocatalytic experiments

The photocatalytic experiments were performed in a cylindrical glass reactor [22, 30, 31]. The volume of the aqueous suspensions was 250 ml. The catalyst concentration was 1 g dm^{-3}. The initial drugs concentration was 50 ppm for *Paracetamol* and 25 ppm for *Cloramphenicol*. The suspensions were first stirred in complete darkness for 30 min to reach sorption-desorption equilibrium of the drugs molecules onto the catalysts surface. After that the illumination was started to carry out the photocatalysis. The source of irradiation was 18 Watt fluorescent BLB UV-A lamp emitting mainly in the region of 340-360 nm. The lamp was fixed at 9 cm above the solution and the UV-light enters the suspension across its interface with the air. The intensity of irradiation at the suspensions surface was 0.014 W/cm^2. Aliquot samples of 5 ml were taken at determined time intervals (UV lamp switched off), centrifuged and then filtered through 0.22 μm membrane filters for complete removal of

the catalyst particles. The drugs concentration in each aliquot was determined at the maximum of pharmaceutical drugs absorbance (243 nm for *Paracetamol* and 278 nm for *Cloramphenicol*) by spectrophotometer Evolution 300 Thermo Scientific (range 200 - 500 nm). After measurement each aliquot, together with the photocatalyst particles, was returned to the treated suspension. All photocatalytic tests were performed at room temperature 23±2°C. Stirring (350 rpm) was kept constant along the experiments to assure oxygen saturation, uniform access of UV light and constant transfer rate of the contaminants to the catalyst surface. The pH of the investigated suspensions, determined by pH meter Hanna instruments, was found to be in the range of 5.7–6.4.

RESULTS AND DISCUSSION

The surface morphology of pure and Ln-modified ZnO powders, observed by SEM, is presented in Figure 2. The micrographs indicate that the modified (La, Ce and Eu) ZnO catalysts are similar, flower-like in shape. The average particle size of 0.4–0.45 µm for modified ZnO, determined from the SEM images, is greater than that of pure ZnO – about 0.25 µm.
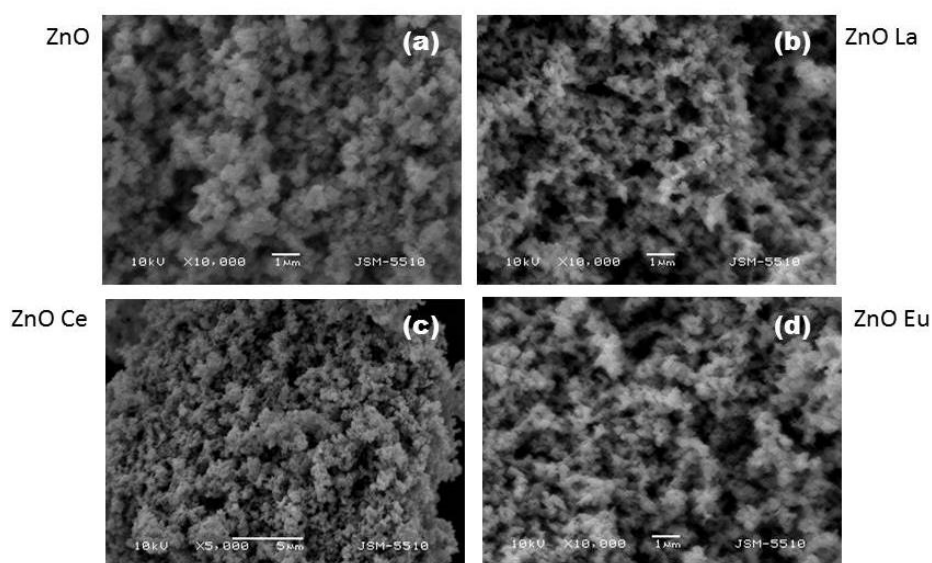

Fig. 2. SEM images of pure ZnO (a) and 2 mol% Ln-modified: La-ZnO (b); Eu-ZnO (c); Ce-ZnO (d) powders.

Fig. 3a, b and c represent EDX analysis of Ln-modified ZnO powder samples and their corresponding X-ray diffraction spectra (Fig. 3d-f). The obtained results from EDX confirm the presence of the dopants La, Ce and Eu onto the surface of catalysts particles. The absence of extra peaks, except the expected ones in the EDX spectrum, shows that the prepared modified (La, Ce and Eu) ZnO catalysts have no impurities. The JCPDS database (Powder Diffraction Files, Joint Committee on Powder Diffraction Standards, Philadelphia PA, USA, 1997) was used to identify the crystal phase composition of the powder samples. The main diffraction peaks (100), (002) and (101) of the samples indicate that ZnO is present as hexagonal wurtzite crystalline phase (PDF # 80-0075). No characteristic peaks of impurity phases like $Zn(OH)_2$ are observed. There are very low peaks corresponding to formation of La_2O_3 (PDF # 83-1350), Eu_2O_3 (PDF # 74-1988) and yellowish CeO_2 (PDF # 81-0792), due to the low dopants concentration - 2 mol%. The XRD patterns of all the modified (La, Ce and Eu) ZnO catalysts are similar, which shows that there is no change in the crystal structure. The average crystallite size, calculated from the most intensive peak (101) is $d_{hk}l = 36$ nm for pure ZnO and $d_{hk}l = 43$ nm for modified (La, Ce and Eu) ZnO catalysts.

The increase in crystallite and particle size upon La, Ce and Eu doping can be attributed to formation of Ln–O–Zn bonds on the surface of the Ln-modified samples, which affects the size of crystallites [32]. The latter is favored by the higher electronegativity and the larger ionic radius of RE cations (103 pm for La^{3+} cations, 108 pm for Eu^{3+} cations and Ce^{4+} cations - ionic radius of 100 pm) than 74 pm for Zn^{2+} cataions. The incorporation of Ln cations in ZnO expands its lattice [33, 34].
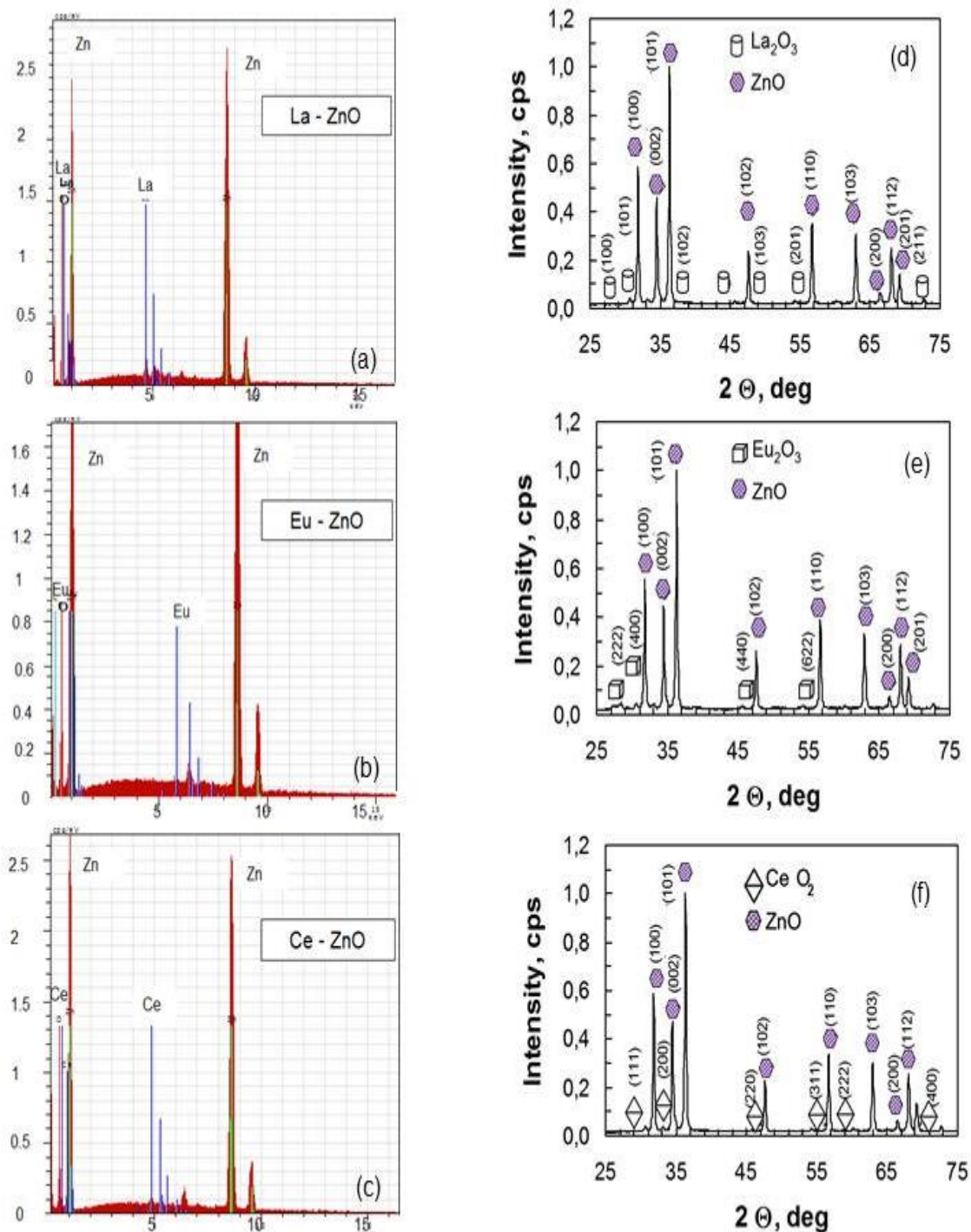
Fig. 3. EDX spectra of ZnO powders modified with La^{3+} (a), Eu^{3+} (b), Ce^{3+} (c) and XRD patterns of La-ZnO (d), Eu-ZnO (e), Ce-ZnO (f) powder photocatalysts.

The surface area of Ln modified powder samples, determined by BET analyses, using N_2 adsorption is found to be 32.34 m^2/g for La, 31.43 m^2/g for Ce and 31.74 m^2/g for Eu modified catalyst. The surface area of modified catalysts is greater in comparison to that of pure ZnO - 10.30 m^2/g.

The photocatalytic activity of Ln (2 mol %) modified ZnO powders towards decomposition of the model pharmaceutical contaminants, *Paracetamol* and *Chloramphenicol*, under UV light

irradiation is compared in Figure 4 and 5. The heterogeneous photocatalytic process is commonly approximated to pseudo-first-order reaction with respect to the contaminant and can be described following the equation:

$$\ln(C_t/C_{in}) = -kt \qquad (2)$$

Here C_{in} is the initial concentration of drugs solution, C_t is the drugs concentration at irradiation time t, and k is the rate constant of photocatalysis.

The solid lines in Fig. 4 are linear fits of the experimental data points by Eq. 2. The slope of logarithmic scale linear fits represents the rate constant of photocatalysis *k*. The corresponding rate constants values *k* of photocatalysis for all samples are also presented in Fig. 4. As seen from the presented data the Ln modified catalysts faster degrade *paracetamol* (Fig. 4a) than *chloramphenicol* (Fig. 4b), despite to its higher initial concentration - 50 ppm for PCA and 25 ppm for CA. In both drugs photodestruction the best result is achieved with the doped with La sample:
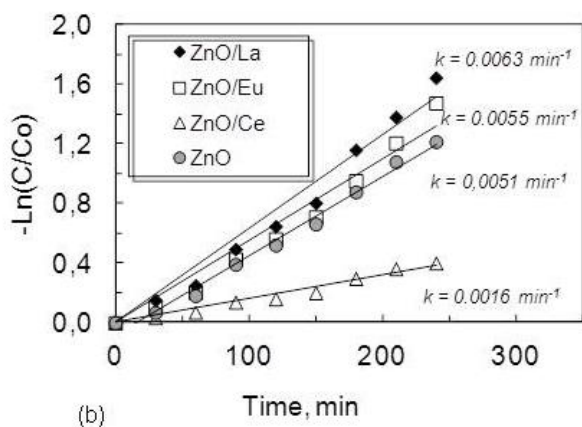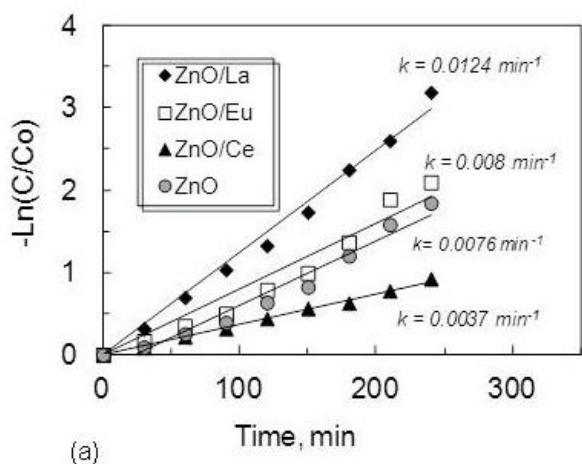
k_{PCA} = 0.01264 min^{-1} and k_{CA} = 0.0063 min^{-1}. The lowest photocatalytic activity shows Ce – modified ZnO sample. These experimental results are confirmed by the degree of photocatalytic mineralization of the drugs (*D%*) (Fig. 5), calculated by the equation:

$$D\% = (C_{in} - C_t)/C_{in} \times 100 \qquad (3)$$

Where C_{in} is the initial drugs concentration and C_t is the concentration of pharmaceutical pollutant after selected moment of illumination time *t*.
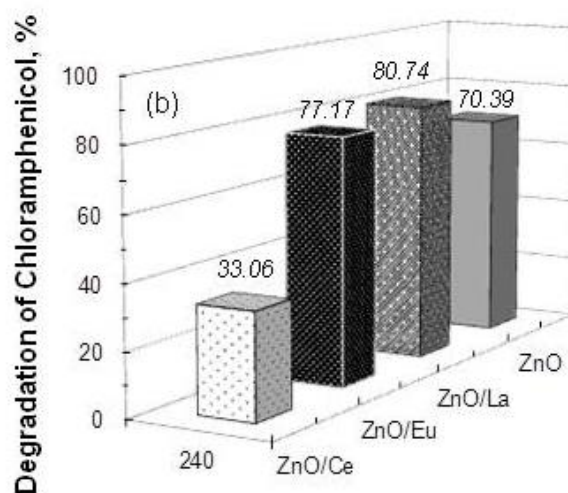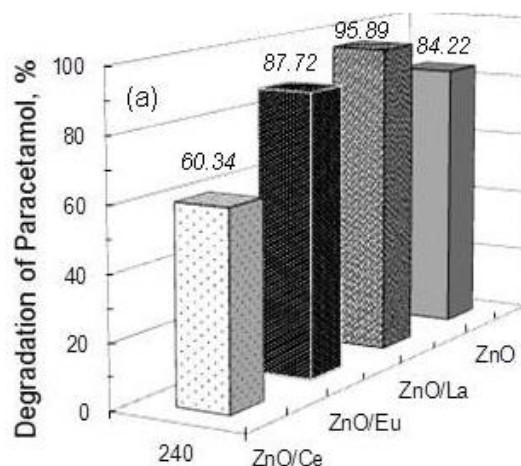

Fig. 4. Kinetics of the photocatalytic degradation of *Paracetamol* (a) and *Chloramphenicol* (b) from aqueous solutions under UV illumination in the presence of pure ZnO and different Ln-modified ZnO powder catalysts.

Fig. 5. Photomineralization degree of *Paracetamol* (a) and *Chloramphenicol* (b) by Ln-modified ZnO powders. The data correspond to 240 min UV light illumination time.

The data in Fig. 5 correspond to 240 min UV light irradiation time. The ZnO powders, doped with La show highest degradation degree of pharmaceuticals (D_{PCA} = 95.88 % and D_{CA} = 80.74 %). The samples prepared by Eu doping have higher (D_{PCA} = 87.72 % and D_{CA} = 60.34 %) photocatalytic efficiency in comparison to these, modified with Ce (D_{PCA} = 77.17 % and D_{CA} = 33.06

%). In accordance to the experimental data, the photodegradation efficiency of doped ZnO powders follows the order La>Eu>Ce. This trend is observed in the course of degradation of both drugs (PCA and CA).

The expected mechanism of photocatalysis with Ln modified ZnO is connected to the possibility for energy transfer between the introduced rare earth

ion energy levels and the conduction/valence band of host ZnO photocatalyst. The 4f-shele of an Ln ion can accept or donate e^- from or to the energy bands of the host with the reactions of valence change such as: $Ln^{3+} + e^- \rightarrow Ln^{2+}$ (for La and Eu) or $Ln^{4+} + e^- \rightarrow Ln^{3+}$ (in case of Ce).

The high efficiency of La and Eu modified ZnO samples can be explained with successful charge separation and production of free radicals. La modified ZnO manifests highest efficiency, which can be attributed to highest number of oxygen vacancies in this case (reasoned by the different charge and electronegativity of La and Zn ions) and as a result – stronger adsorption of OH^- ions onto the catalysts surface. The latter favors the formation of •OH by reaction of h^+ and OH^-. The •OH radicals are extremely strong non-selective oxidants, which degrade the organic molecules at the surface of La modified ZnO. In case of Eu modified ZnO the introduced Eu energy levels are close, but lower to the energy of ZnO conduction band, which favors formation of $•O_2^-$ radicals by reaction of photogenerated e^- and O_2. In case of Ce modified ZnO the reverse process (transferring of e^-) is forbidden, which leads to deep e^- trapping and the observed low photocatalytic efficiency of Ce-modified ZnO sample.

The prepared Ln modified ZnO photocatalysts seem promising for the purification of drugs contaminated wastewaters.

CONCLUSIONS

Ln modified (2 mol %) ZnO powders are prepared by thermal method. Their structural and photocatalytic properties have been established. It's experimentally found that Ln-ZnO powders achieve faster degradation of PCA, compared to that of CA under UV-light irradiation. Higher degradation efficiencies are encountered for the modified with La ZnO powders, degradation efficiency values of 95.88% (PCA) and 80.74% (CA) are observed after 240 min of photocatalytic treatment. With Eu3+ the following removal efficiencies are obtained: 87.72% (PCA) and 77.17% (CA). The modified powders with Ce^{3+} have the lowest photocatalytic efficiency. The high efficiency of La and Eu modified ZnO samples can be explained with successful charge separation and production of free radicals.

REFERENCES

1. A.J. Ebele, M A-E Abdallah, S Harrad, *Emerging Contaminants*, **3**, 1 (2017).
2. A. Sangion, P. Gramatica, *Environ. Int.*, **95**, 131 (2016).
3. A.W. Garrison, J.D. Pope, F. Allen, Identification and Analysis of Organic Pollutants in Water. In: Ann Arbor Science Publishers, Keith, L.H. (Ed.), Ann Arbor Science, 1976, 517–556.
4. C. Hignite, D.L. Azarnoff. *Life Sci.*, **20**, 337 (1977).
5. M. Ezechias, J. Janochova, A. Filipova, Z. Kresinova, T. Cajthaml, *Chemosphere*, **152**, 284 (2016).
6. L.H.M.L.M. Santos, A.N. Araújo, Adriano Fachini, A. Pena, C. Delerue-Matos, M.C.B.S.M. Montenegro, *J. Hazardous Mater.*, **175**, 45 (2010).
7. H.-J. Son. Seong, S.H, Jang, *J. Korean Soc. Environ. Engrs*, Review Paper 453 (2011). DOI: 10.4491/KSEE.2011.33.6.453
8. M.G. Lusk, G.S. Toor, Y.-Y. Yang, S. Mechtensimer, M. De, T.A. Obreza, *Critical Rev. Enviro. Sci. Technol.*, **47**, 455 (2017). DOI: 10.1080/10643389.2017.1327787
9. A. Nikolaou, S. Meric, D. Fatta, *Anal. Bioanal. Chem.*, **387,** 1225 (2007).
10. N. Abedi, A. Nabi, E. Mangoli, A.R. Talebi, *Middle East Fertility Soc. J.*, **22**, 323 (2017).
11. A. Puckowski, K. Mioduszewska, P. Łukaszewicz, M. Borecka, M. Caban, J. Maszkowska, P. Stepnowski, *J. Pharm. Biomed. Analysis*, **127**, 232 (2016).
12. L. Connolly, E. Ropstad, S. Verhaegen, *Trends Anal. Chem.*, **30**, 227 (2011).
13. Z. Wei, N.W. Kelsey, H. Nancy, A.D. Nathan, R.S. Clinton, Uptake, Translocation, and Accumulation of Pharmaceutical and Hormone Contaminants in Vegetables. Retention, Uptake, and Translocation of Agrochemicals in Plants, American Chemical Society, 2014.
14. E. Wielogorska, C.T. Elliott, M. Danaher, O. Chevallier, L. Connolly, *Food Control.*, **48**, 48 (2015).
15. D. Kanakaraju, Beverley D. Glass, Michael Oelgemoller, *J. Environ. Manag.*, **219**, 189 (2018).
16. S. Carbonaro, M.N. Sugihara, T.J. Strathmann, *Appl. Catal. B Environ.*, **129**, 1 (2013).
17. O.K. Dalrymple, D.H. Yeh, M.A. Trotz, *J. Chem. Technol. Biotechnol.*, **82**, 121 (2007).
18. P. Calza, V.A. Sakkas, C. Medana, C. Baiocchi, A. Dimou, E. Pelizzetti, T. Albanis, *Appl. Catal. B Environ.* , **67**, 197 (2006).
19. J.P. Candido, S.J. Andrade, A.L. Fonseca, F.S. Silva, M.R.A. Silva, M.M. Kondo, *Environ. Sci. Pollut. Res.*, **23**, 19911 (2016).
20. M.A. Hernández-Carrillo, R. Torres-Ricárdez, M.F. García-Mendoza, E. Ramírez-Morales, G. Pérez-Hernández, *Catalysis Today* in press. https://doi.org/10.1016/j.cattod.2018.04.060

21. N. Kaneva, A. Bojinova, K. Papazova, *J. Phys. Conf. Ser.*, **682**, 012022 pdf (2016) doi:10.1088/1742-6596/682/1/012022.
22. N. Kaneva, A. Bojinova, K. Papazova, D, Dimitrov, *Catalysis Today*, **252** 113 (2015).
23. N. Kaneva, A. Bojinova, K. Papazova, D, Dimitrov, A. Eliyas, *Bulg. Chem. Commun*., **49**, 172 (2017).
24. S. Vitols, *J. Intern. Med.*, **253**, 95 (2003).
25. J. Kurtovic, S.M. Riordan, *J. Intern. Med.*, **253**, 240 (2003).
26. K. Ajit, A. Sarmah, M. Meyer, A. Boxall, *Chemosphere*, **65**, 725 (2006).
27. I. Liphshitz, A. Loewenstein, *Br. J. Ophthalmol*., **75**, 64 (1991).
28. C. Diskin, *Mayo. Clin. Proc.*, **80**, 1392 (2005).
29. K. Woodward (2004) In: Watson, D.H. (Ed.) Pesticide, Veterinary and Other Residues in Food. Woodward Publisher Limited, Cambridge, 176 (Chapter 8).
30. S. Siuleiman, N. Kaneva, A. Bojinova, D. Dimitrov, K. Papazova, *Bulg. Chem. Commun*., **49** (G), 199 (2017).
31. S.A. Syuleiman, N.D. Yakushova, I.A. Pronin, N.V. Kaneva, A.S. Bojinova, K.I. Papazova, M.N. Gancheva, D.Tz. Dimitrov, I.A. Averin, E.I. Terukov, V.A. Moshnikov, *Technical Physics*, **62**, 1709 (2017).
32. J. Lin, J.C. Yu, D. Lo, S.K. Lam, *J. Catal*. **183**, 368 (1999).
33. A.F. Wells, "Structural Inorganic Chemistry," 5th ed., Clarendon Press, Oxford, 1984, p. 1288.
34. C.L. Muhich, *J. Phys. Chem. C*, **121**, 8052 (2017).